ИНДЕКС 3649

ЕРЕВАНСКИЙ ФИЗИЧЕСКИЙ ИНСТИТУТ

Preprint YPI-1384(14)-92

ԵՐԵՎԱՆԻ ՖԻԶԻԿԱՅԻ ԻՆՍՏԻՏՈՒՏ
ЕРЕВАНСКИЙ ФИЗИЧЕСКИЙ ИНСТИТУТ
YEREVAN PHYSICS INSTITUTE

Ts. A. Amatuni, E. A. Hamidjanjan and Kh. M. Sanossyan

Monte-Carlo Simulation of Hadronic Showers

Part 4. The ANI Calorimeter

ЦНИИатоминформ
Ереван 1992

Препринт ЕФИ-1384(14)-92

Ц. А. Анатуни, Э. А. Мамидханян, Х. Н. Сависян

МОДЕЛИРОВАНИЕ АДРОННЫХ ЛИВНЕЙ МЕТОДОМ МОНТЕ-КАРЛО

ЧАСТЬ 4: КАЛОРИМЕТР ЭКСПЕРИМЕНТАЛЬНОГО КОМПЛЕКСА "АНИ"

Моделированы адронные ливни, инициированные 1, 5, 10, 20, 50 и 100ТэВ-ными протонами, налетающими на калориметр экспериментального комплекса "АНИ" используя программу MARS10. Представлены продольные и поперечные профили этих ливней. Оценен пронос из калориметра "АНИ".

ЕРЕВАНСКИЙ ФИЗИЧЕСКИЙ ИНСТИТУТ

ЕРЕВАН 1992

1. The Experimental Setup.

The ANI facility [1-3] is a unique set of installations on mountain Aragads (3250m above sea level) designed for the investigation of hadron and nucleus interactions in the 10^2-10^5 TeV energy range, primary cosmic radiation in that energy range and gamma astronomy.

The ANI facility consists of the following main components: an ionization calorimeter, scintillation hodoscopes[4,5], Air Cherenkov detectors [4,6,7], underground muon detectors("ANI-Magnet") [8-12], the PION calorimeter [13-15], the ANI-Prototype [16,17] and cosmic ray intensity variation detectors (18-NM-64 type neutron supermonitors). The central part of the ANI facility is intended for the investigation of the space-time and energy characteristics of the EAS core.

The layout of the central part of the ANI calorimeter consists of figure 4.1. The overground part of the ANI calorimeter consists of three sections: the gamma section - for detection and identification of high energy (above 2TeV) gamma ray families; the hadronic section - for the determination of high energy hadron coordinates in the EAS core ; and the ionization calorimeter - for hadronic shower detection. The sequence of materials up to foundation level (over the central underground experimental hall) is given in Table 4-1. As it is seen from the table the overall depth of absorber is Z_{max}=1195cm and amounts to 1304.15g/cm^2. The surface of the calorimeter is 40x40m^2.

The gamma-section consists of two layers of X-ray films (one of them is fixed, the other can be moved over it) placed over blowing pillows, two layers of ionization chambers (IC) and two layers of lead absorbers each 3cm thick. The first row of IC is placed under the first lead absorber, the second row of IC is placed under the X-ray films

which are under the second layer of lead absorber. 29.4cm wide air gaps exist under each IC layer (see fig. 4.1 a)). The PT-6M type X-ray film is double sided with 200 micron thickness and allows to define the incidence angles of the γ-quanta. The wide density range combined with an appropriate measurement method allows one to define the energy of single γ-quanta up to ~100TeV. The position resolution is ~10 μm [18]. The conjunction of fixed and moving X-ray film layers allows to put in correspondence the γ-quanta and γ-quanta families with the extensive air showers detected by the other (electronic) parts of the ANI setup. The ionization chambers allow to measure the energy flux carried by electrons and photons with energies less than 2TeV which will be absorbed in the lead absorbers and to reconstruct together the events detected by the calorimeter and the X-ray films. The ionization chambers are made of 3mm steel with dimensions 10cm X 14cm X 600cm and are filled with argon at 3 atm.

The hadronic section consists of a 45cm thick carbon layer and 3cm lead plate which serves as a target for hadron interaction, one layer of X-ray film, 2cm iron plate and one row of IC, after which remains yet another 29.4cm wide air gap. There is a 135cm empty gap between the γ-section and the h-section aimed for installation of an additional module in the future.

The ionization calorimeter consists of 7 modules each of which includes a 60cm layer of standard composition concrete, a 2cm iron plate, a row of ionization chambers of the same construction as above and a 29.4cm wide air gap. The IC in the alternating layers of the calorimeter as well as in the γ- and h-sections are located in perpendicular directions which allows to estimate the coordinates of the EAS core.

2. Cascade Simulations

The Monte-Carlo simulation of the central part of the ANI facility were carried out with the help of the MARS10 code[19-21]. The code was written by N. V. Mokhov in mid 70-ies and has been extensively modified and tested by the IHEP (Serpukhov) group over the past years. A weighted Monte-Carlo algorithm is used in MARS, so that only the average characteristics of the shower can be estimated. Typical computing times are of the order of an hour and vary logarithmically with the incident energy.

In MARS10 the tabulated values of hadron-nucleus interaction

cross sections are used for $E_0 \leq$ 20TeV. The simulations for the incident energies above 20TeV were carried out using the same interaction cross sections as for 20TeV. The simulations were performed in cylindrical geometry with the Z-axis pointed downwards and the origin at the middle of the calorimeter upper surface.The energy cutoff was 10MeV. The number of simulated showers per each primary energy was 5000. The primaries were incident protons along the Z-axis. Hadron cascades were calculated for 1, 2, 5, 10, 15, 20, 30, 50 and 100TeV primary energies.

The computer time needed for shower simulation increases substantially with the complexity of the absorber geometry. To save time we have "added" the 2cm iron plates to the concrete layers by weight, recalculating the composition and density of the latter. This had practically negligible influence on the results but made the simulations much faster (of the order of several hours per incident energy on a BESM-6 computer).

The total laterally integrated energy deposition in concrete as a function of ionization calorimeter module number for 1, 5, 10, 20, 50 and 100TeV primary proton induced showers are given in fig. 4.2. The total laterally integrated energy deposition in the active absorber layers(argon) as a function of ionization calorimeter module number for the same showers are given in fig. 4.3. Longitudinally integrated (from 0 to Z_{max}) reduced lateral profiles -

$$1/E_{tot}(\Delta E_{tot}/\Delta R),$$

where

E_{tot} - is the total deposited energy,

ΔE_{tot} - is total deposited energy in the cylindrical ring of thickness ΔR,

R - is distance from the shower axis, for 1, 5, 10 and 20TeV primary proton energies are given in fig. 4.4. The lateral reduced profiles at the cascade maximum -

$$1/E_{max}(\Delta E_{max}/\Delta R),$$

where

E_{max} - is deposited energy in the layer of maximum,

ΔE_{max} - is deposited energy in the layer of maximum within [R, R+ΔR], for 1, 5, 10 and 20TeV primary proton induced showers are given in fig. 4.5. The reduced lateral profiles in the 4-the concrete layer (middle) -

$$1/E_4(\Delta E_4/\Delta R),$$

where

E_4 – is deposited energy in the 4-th layer,

ΔE_4 – is deposited energy in the 4-th layer within [R, R+ΔR], for 1, 5, 10 and 20TeV primary proton induced showers are given in fig. 4.6. The energy deposition in the active absorber of the ionization calorimeter ($\Sigma_{i=1}^{7} \hat{E}_i^{Ar}$) as a function of primary energy is presented in Table 4–2 and in fig. 4.7. It can be fitted by the following formula:

$$\hat{E}(\text{GeV}) = 0.49(\pm 0.02)E_0(\text{TeV}), \qquad (4.1)$$

where E_0(in TeV) is the primary proton energy and χ^2=0.91.

The leakage energy and the number of leakage particles for 1, 2, 5, 10, 15, 20, 30, 50 and 100TeV proton induced showers are presented in Table 4–3. The energy dependence of the total leakage energy is given in fig. 4.8. The energy dependence of the forward leakage energy for the above mentioned cascades is presented in fig. 4.9. It can be fitted by the following formula:

$$\hat{E}_{F.-w.L.}(\text{GeV}) = 18.90(\pm 1.46)E_0(\text{TeV}). \qquad (4.2)$$

The energy dependence of the number of forward leakage particles for mentioned showers is presented in fig. 4.10. It can be fitted by the following formula:

$$\hat{N}_{F.-w.L.} = 20.11(\pm 1.41)\, E_0(\text{TeV}). \qquad (4.3)$$

The r.m.s. errors of the calculated values in (4.2) and (4.3) is considered to be 20%.

ACKNOWLEDGEMENTS

We would like to thank our colleagues from the Cosmic Ray Department for many useful and stimulating discussions.

TABLES

Table 4–1. The sequence of materials with corresponding thickness and density in the ANI setup.

Depth		ΔZ	ρΔZ	Medium
cm	g/cm²	cm	g/cm²	
3.	34.032	3.	34.032	Pb
3.3	36.39	0.3	2.358	Fe
13.3	36.4434	10.	0.0534	Ar (at 3atm.)
13.6	38.8014	0.3	2.358	Fe
43.	38.8393	29.4	0.03793	Air
46.	72.8713	3.	34.032	Pb
61.	72.8907	15.	0.01935	Air
61.4		0.4		Fe
61.7	78.3927	0.3	5.502	Fe
71.7	78.4461	10.	0.0534	Ar(at 3atm.)
72.	80.8041	0.3	2.358	Fe
101.4		29.4		Air
236.	81.0156	134.6	0.2116	Air
281.	157.9656	45.	76.95	Carbon
284.	191.9976	3.	34.032	Pb
291.	192.0067	7.	0.00903	Air
293.	207.7267	2.	15.72	Fe
303.	207.78	10.	0.0534	Ar(at 3atm.)
332.4	207.818	29.4	0.03793	Air
395.	364.318	62.6	156.5	Concrete
405.	364.3714	10.	0.0534	Ar(at 3atm.)
434.4	364.4093	29.4	0.03793	Air
497.	520.9093	62.6	156.5	Concrete
507.	520.9627	10.	0.0534	Ar(at 3atm.)
536.4	521.0007	29.4	0.03793	Air
599.	677.5007	62.6	156.5	Concrete
609.	677.5541	10.	0.0534	Ar(at 3atm.)
638.4	677.592	29.4	0.03793	Air
701.	834.092	62.6	156.5	Concrete
711.	834.1454	10.	0.0534	Ar(at 3atm.)
740.4	834.1833	29.4	0.03793	Air
803.	990.6833	62.6	156.5	Concrete

Table 4-1. (Continuation)

1	2	3	4	5
813.	990.7367	10.	0.0534	Ar(at 3atm.)
842.4	990.7746	29.4	0.03793	Air
905.	1147.2747	62.6	156.5	Concrete
915.	1147.3281	10.	0.0534	Ar(at 3atm.)
944.4	1147.366	29.4	0.03793	Air
1007.	1303.866	62.6	156.5	Concrete
1017.	1303.9194	10.	0.0534	Ar(at 3atm.)
1195.	1304.149	178.	0.22962	Air
The Foundation Level				

Table 4-2. Energy deposition in active part of calorimeter, GeV.

E_0, TeV	$\mathcal{E} = \Sigma_{i=1}^{7} E_i^{Ar}$	$\Delta\mathcal{E}$	$\hat{\mathcal{E}}$
1	0.67	0.105	0.49
2	1.14	0.18	0.97
5	2.57	0.26	2.43
10	4.68	0.7	4.86
15	6.59	0.52	7.3
20	9.84	0.77	9.73
30	13.28	1.91	14.59
50	23.94	3.53	24.32
100	53.28	5.7	48.64

Table 4-3. Leakage from the ANI calorimeter.

Incident Energy, TeV	Leakage Energy, GeV: Hadrons: Backward	Hadrons: Forward	Hadrons: Side	Low-Energy Neutrons	Photons and Electrons	Total	Number of Leakage Particles: Backward	Forward	Side
1	0.30	14.	1.01	0.04	4.	20.	5.	17.	13.
2	0.37	50.	1.45	0.04	9.	61.	7.	69.	17.
5	0.60	85.	3.55	0.06	27.	117.	9.	72.	49.
10	0.44	255.	228.5	0.08	68.	553.	9.	238	1613.
15	0.77	416.	7.27	0.21	147.	571.	12.	614.	67.
20	0.94	534.	6.33	0.07	207.	749.	22.	450.	79.
30	0.39	773.	5.91	0.08	228.	1007.	8.	851.	61.
50	1.84	2052.	8.44	0.16	844.	2906.	41.	1317.	103.
100	0.64	2077.	12.54	0.93	702.	2791.	14.	1605.	163.

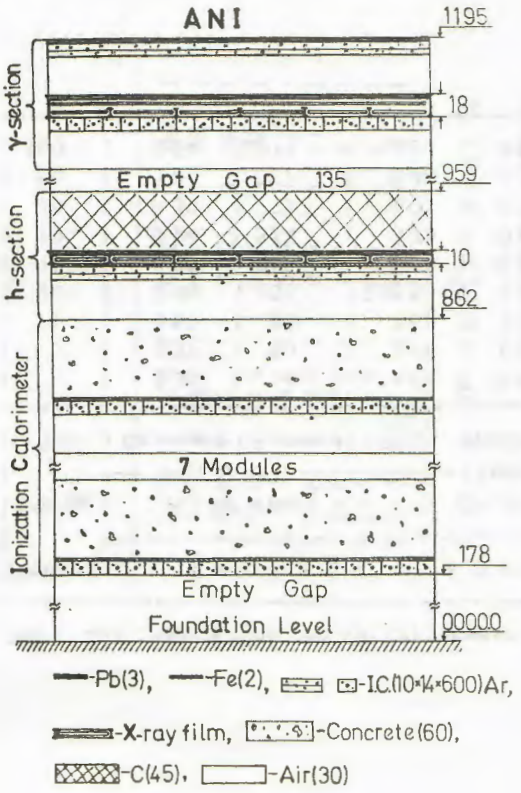

Fig. 4.1 a)

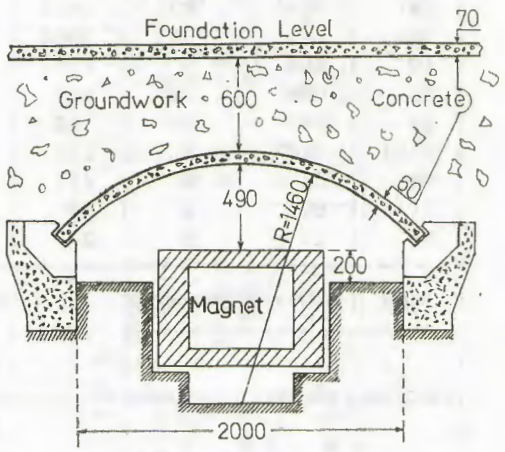

Fig. 4.1 b)

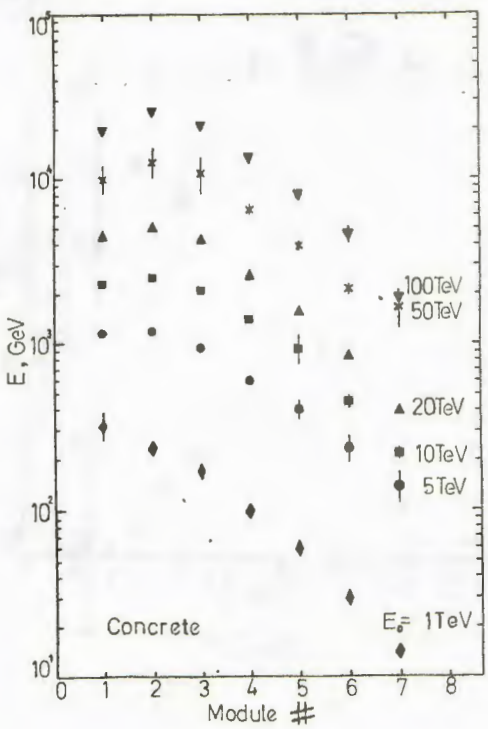

Fig. 4.2

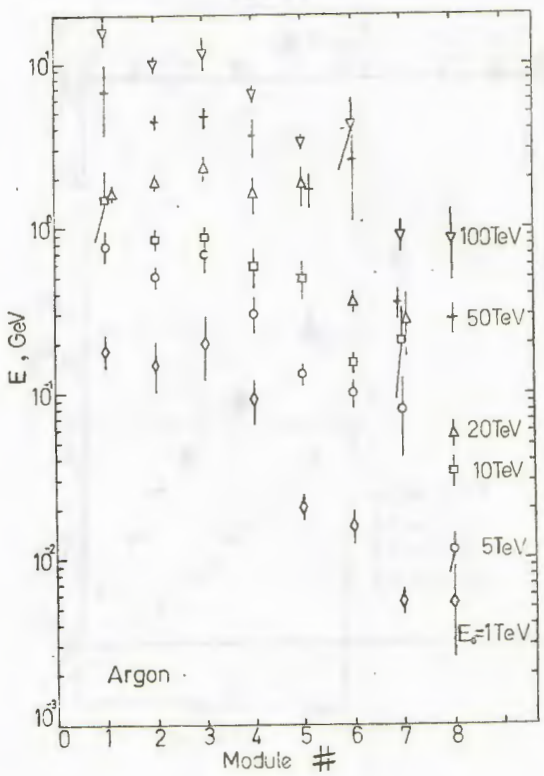

Fig. 4.3

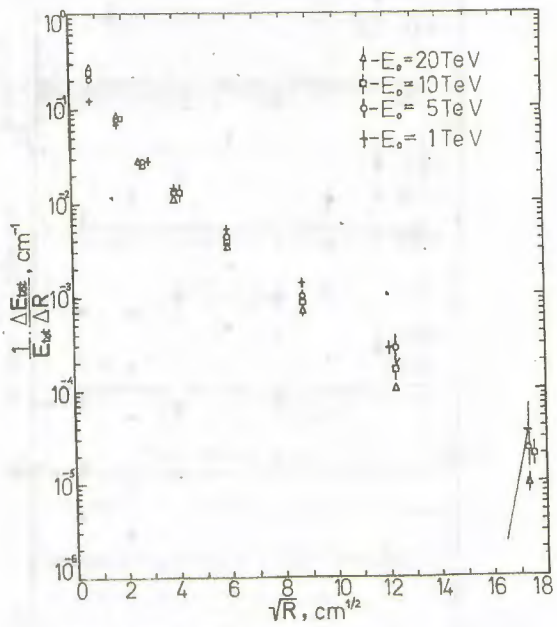

Fig. 4.4

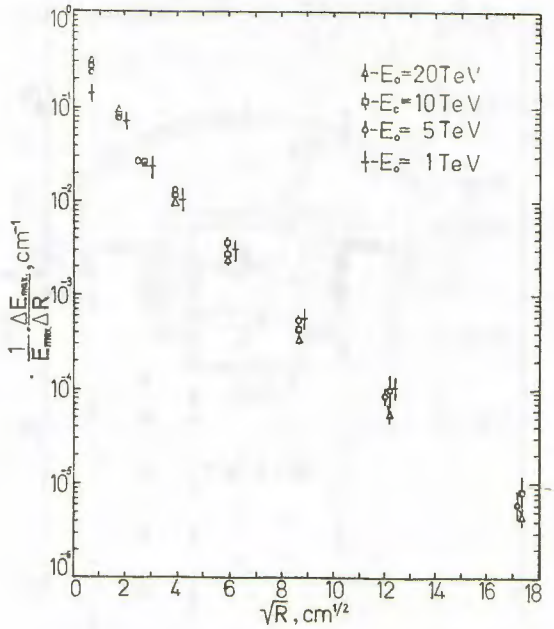

Fig. 4.5

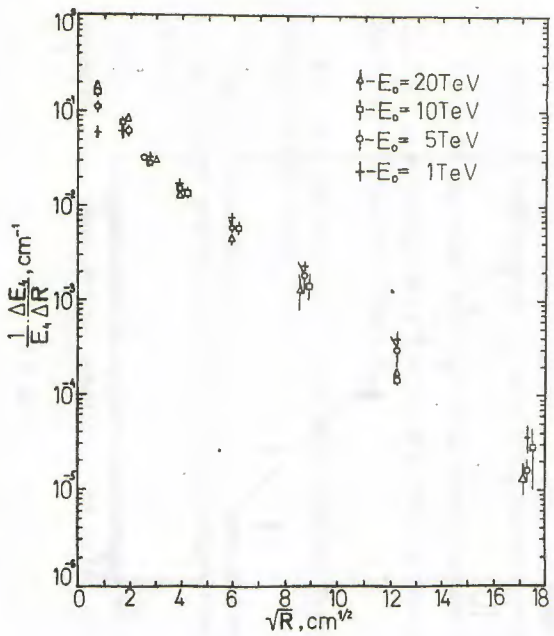

Fig. 4.6

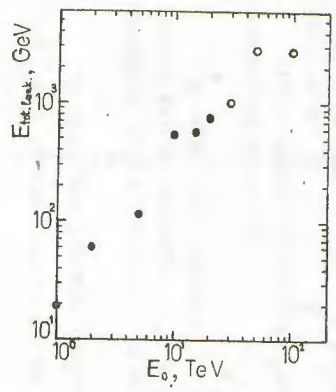

Fig. 4.8

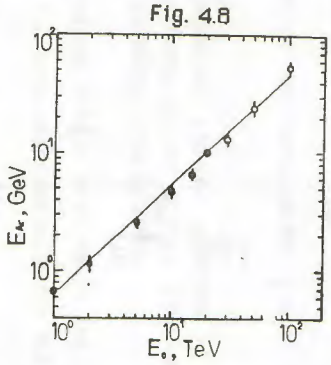

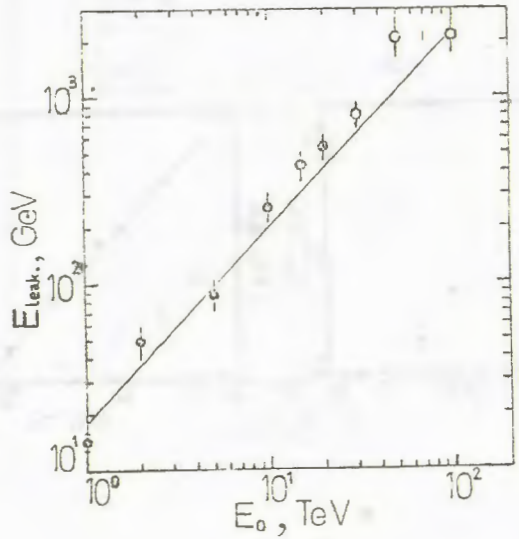

Fig. 4.9

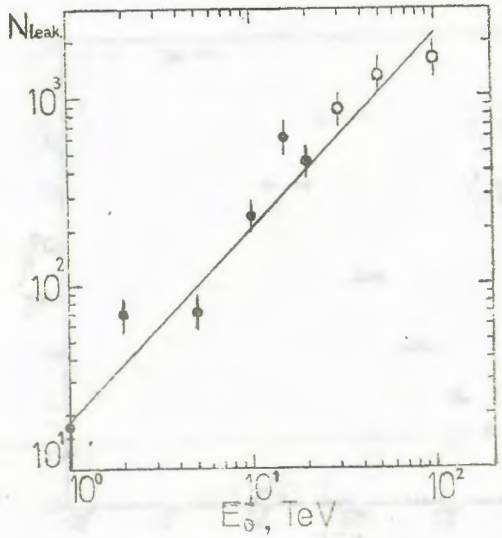

Fig. 4.10

FIGURE CAPTIONS

Fig. 4.1. a) The layout of the ANI setup above ground. The dimensions are in cm. The sequence of materials is presented in Table 4-1.

b)The layout of central part of ANI setup under ground. The dimensions are in cm.

Fig. 4.2. The average longitudinal shower profiles in the concrete+iron absorber. E_0-is primary proton energy. The cutoff energy is 10MeV, the number of shower histories is 5000.

Fig. 4.3. The average longitudinal shower profiles in the IC-s ($in\sum_{i=1}^{7}Ar_i$) of ANI calorimeter for the same cascades as in fig. 4.2.

Fig. 4.4. Longitudinally integrated (from 0 to Z_{max}) reduced lateral shower profiles. E_0-is primary proton energy.

Fig. 4.5. Reduced lateral shower profiles at the showers' maxima. E_0-is primary proton energy.

Fig. 4.6. Reduced lateral profiles in the 4-th (concrete) layer of the ionization calorimeter. E_0-is primary proton energy.

Fig. 4.7. Dependence of the total energy deposition in the IC-s ($\sum_{i=1}^{7}E_i^{Ar}$) on primary energy. Circles are MARS10 results, the straight line is χ^2 fit. See also Table 4-2.

Fig. 4.8. Dependence of the total leakage energy on incident energy. See also Table 4-3.

Fig. 4.9. Dependence of the forward leakage energy on incident energy. Circles are MARS10 results, the straight line is fit. See also Table 4-3.

Fig. 4.10. Dependence of the average number of forward leakage particles on incident energy. Notations - as in fig. 4.9. See also Table 4-3.

REFERENCES

[1] A. Ts. Amatuni, E. A. Mamidjanyan, S. H. Matinyan et al., Preprint YerPI-358(16)-79, Yerevan, 1979 (in Russion).

V. V. Avakyan et al., Uspekhi Physicheskikh Nauk, v. 132, 395 (1980) (in Russion).

[2] V. V. Avakyan et al., Izvestiya AN Arm. SSR, Seriya Physika, v. 17, Vipusk 3-4, 129-232 , Yerevan, 1982 (in Russion).

[3] E. A. Mamidjanyan and S. I. Nikolski, Preprint YerPI-1301(87)-90, Yerevan, 1990 (in Russion).

[4] V. V. Avakyan, A. T. Havoundjyan, S. A. Aghadjanyan et al., Voprosi Atomnoy Nauki i Tekhniki (VANT), Seriya: Tekhnika Physicheskogo Experimenta (TPE), 2(33), 12, Yerevan, 1987 (in Russion).

[5] Yerevan - Lebedev Physics Institute collaboration, Proc. of the 18th ICRC, Bangalore, 1983, v.5, p. 520.

[6] S. A. Aghadjanyan, F. A. Aharonyan, A. Ts. Amatuni et al., Proc. of the 20th ICRC, Moscow, 1987, OG 9.1 - 18.

[7] F. A. Aharonyan, Thesis, YerPI, Yerevan, 1988.

[8] T. L. Asatiani, V. A. Ivanov and E. A. Mnatsakanyan, VANT, Seriya: TPE, 2(8), 77, Yerevan, 1981 (in Russion).

[9] T. L. Asatiani, V. A. Ivanov and E. A. Mnatsakanyan, Proc. of the 17-th ICRC, v.8, 126, Paris, 1981.

[10] T. L. Asatiani, V. A. Ivanov and E. A. Mnatsakanyan, VANT, Seriya: TPE, 2(8), 82, Yerevan, 1981 (in Russion).

[11] E. A. Mnatsakanyan, S. V. Ter Antonyan and P. A. Martirossyan, Preprint YerPI-1058(21)-88, Yerevan, 1988 (in Russion).

[12] E. A. Mnatsakanyan, Thesis, YerPI, Yerevan, 1989.

[13] V. V. Avakyan et al., VANT, Seriya: TPE, 4(16), 3, Yerevan, 1983 (in Russion).

[14] V. V. Avakyan, Thesis, YerPI, Yerevan, 1988.

[15] Ts. A. Amatuni, E. A. Mamidjanyan and Kh. N. Sanossyan, Part 2 of this work. Preprint YerPI-1382(12)-92, Yerevan, 1992.

[16] V. V. Avakyan et al., VANT, Seriya: TPE, 5(31), 3, Yerevan, 1988 (in Russion).

[17] Ts. A. Amatuni, E. A. Mamidjanyan and Kh. N. Sanossyan, Part 3 of this work. Preprint YerPI-1383(13)-92, Yerevan, 1992.

[18] L. G. Melkoumyan, Thesis, YerPI, Yerevan, 1990.

[19] A. N. Kalinovski, N. V. Mokhov and Yu. P. Nikitin, Passage of High Energy Particles Through Matter, Energoatomizdat, Moscow, 1985, (in Russion).

[20] N. V. Mokhov and J. D. Cossairt, Fermilab Report, FN-424, Fermilab, Batavia, IL. USA, 1985.

[21] Ts. A. Amatuni, E. A. Mamidjanyan and Kh. N. Sanossyan, Part 1 of this work. Preprint YerPI-1381(11)-92, Yerevan, 1992.

The manuscript was received 13th Oct. 1992.

.А.АМАТУНИ, Э.А.КАМИДЖАНЯН, Х.Н.САНОСЯН

ОДЕЛИРОВАНИЕ АДРОННЫХ ЛИВНЕЙ МЕТОДОМ МОНТЕ-КАРЛО
АСТЬ 4: КАЛОРИМЕТР ЭКСПЕРИМЕНТАЛЬНОГО КОМПЛЕКСА "АНИ"

на английском языке)

едактор А.С.Есин
ехнический редактор А.С.Абрамян

одписано в печать 5/ХП-92г. Формат 60x84x16
ечатная печать. Уч.изд.л. I,0 Тираж I00 экз. Ц. 8 р.
ак.тип.065 Индекс 3649

тпечатано в Ереванском физическом институте
реван-36, ул.Братьев Алиханян, 2

The address for requests:
Information Department
Yerevan Physics Institute
Alikhanian Brothers 2,
Yrevan, 375036
Armenia, USSR